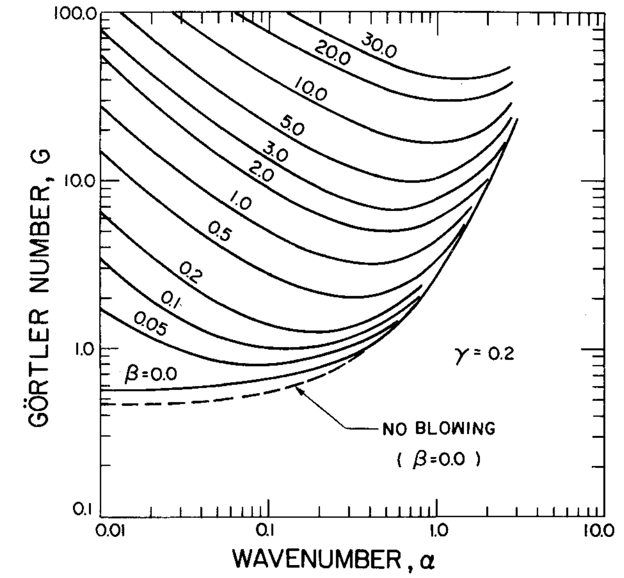

Fig. 2 Curves of constant amplification rate β as a function of Görtler number G and wavenumber α for the Blasius boundary layer with self-similar blowing of $\gamma = 0.2$.

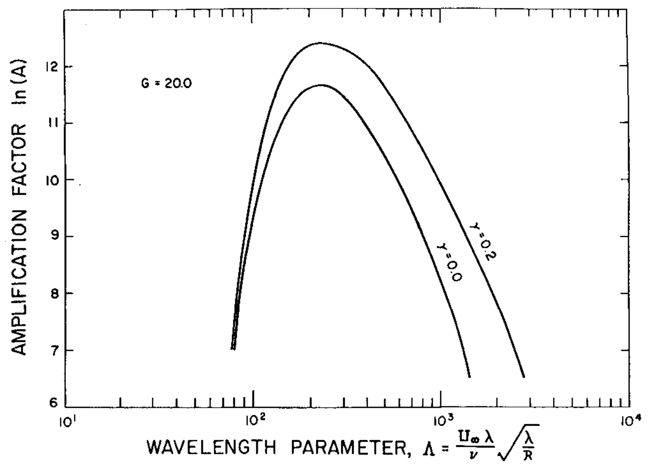

Fig. 3 Curves of total growth of disturbances as a function of the wavelength parameter Λ at the streamwise location corresponding to Görtler number $G = 20.0$. Calculations are for the Blasius boundary layers without blowing and with self-similar blowing of $\gamma = 0.2$.

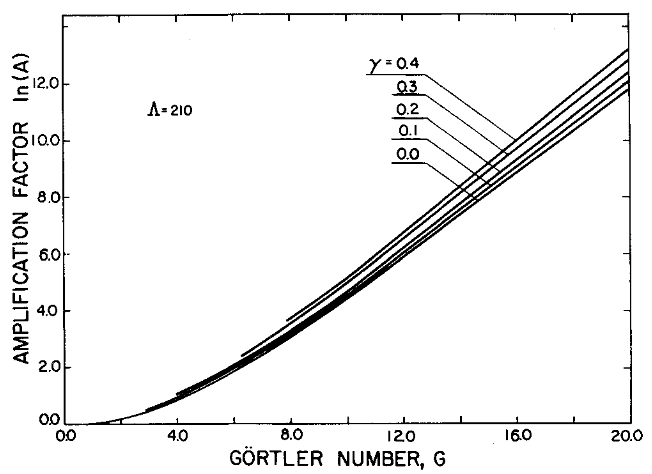

Fig. 4 Curves of total growth of disturbances as a function of Görtler number for the Blasius boundary layer with different levels of self-similar blowing. The value of the wavelength parameter Λ corresponds to the disturbances of the maximum total growth for the no-blowing case.

while it delays the onset of the instability, blowing increases the rate of growth of the disturbances and leads to a higher total amplification. The most amplified disturbances correspond to $\Lambda = 210$ for the no-blowing case[4] and blowing slightly increases this value. Figure 4 illustrates the variations of the total amplification of the disturbances for different levels of blowing as a function of Görtler number for vortices corresponding to $\Lambda = 210$. It may be concluded that while blowing increases the total growth, the growth process is qualitatively unaffected.

Conclusions

The effect of blowing on the Görtler instability of boundary layers has been studied for the case of self-similar blowing. An increase in blowing increases the critical Görtler number; however, it also accelerates the growth of the disturbances and thus may lead to an earlier transition.

Acknowledgment

This work was supported by a grant from the Natural Sciences and Engineering Research Council of Canada. The author would like to thank Mr. S. K. Chua for performing the computations.

References

[1]Floryan, J. M. and Saric, W. S., "Effects of Suction on the Görtler Instability of Boundary Layers," *AIAA Journal*, Vol. 21, Dec. 1983, pp. 1635-1639.

[2]Kobayashi, R., "Taylor-Görtler Instability of a Boundary Layer with Suction or Blowing," *AIAA Journal*, Vol. 12, March 1974, pp. 394-395.

[3]Floryan, J. M. and Saric, W. S., "Stability of Görtler Vortices in Boundary Layers," *AIAA Journal*, Vol. 20, March 1983, pp. 316-324.

[4]Floryan, J. M. and Saric, W. S., "Wavelength Selection and Growth of Görtler Vortices," *AIAA Journal*, Vol. 22, Nov. 1984, pp. 1529-1538.

Statistical Processing of Multiplexed Data from Turbulent Flames

Roger J. Becker*
University of Dayton, Dayton, Ohio

Introduction

MULTICOMPONENT dynamic systems such as flames and turbulent flows are extremely complex. A full understanding of their behavior requires a knowledge of the time dependence of the interactions between the various components of the system. This in turn necessitates the accumulation of a vast store of time-resolved data. It also requires the simultaneous monitoring of two or more system components, which represents a severe experimental challenge. It is often impractical to record simultaneously the behavior of several data records without first multiplexing the data on the various system components. Multiplexing in component space makes a time-dependent analysis more difficult to execute. However, it is not as troublesome as many have supposed.

We know it is possible to obtain the real-time data record of a single spectral component of the data. This record can subsequently be analyzed to obtain statistical functions of the time evolution of a single measured parameter. It is also possible,

Received Oct. 18, 1983; revision submitted July 1984.

*Research Physicist, Research Institute.

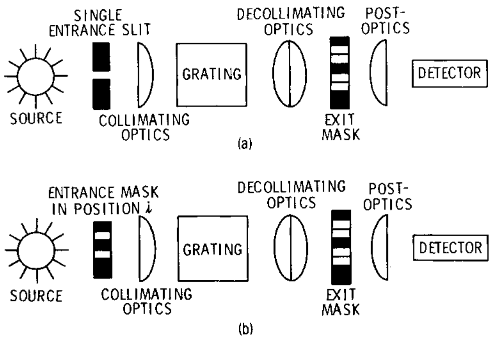

Fig. 1 Detection optics of illustrative real-time data acquisition system. An encoding mask is located at exit plane of spectrometer. All light passing this mask is passed to detector. The source has a random time dependence. The encoding mask is stepped through a sequence of orthogonal encoding patterns.

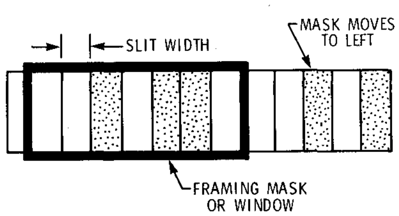

Fig. 2 Typical sequential encoding scheme used in Hadamard transform optics. Light is accepted only over the aperture of the framing window. As the mask is stepped by one slit width, a new, orthogonal encoding mask is obtained. (From Ref. 1.)

at least in principle, to multiplex the data spectrally and obtain the time-averaged behavior of several spectral components of the data. This can be accomplished by a suitable spectral transforming filter, such as a Hadamard transform.[1] We now show that it is also possible to obtain statistical data from random, stationary processes that are both time-resolved and spectrally multiplexed. The power of such an analysis offers a large jump in both efficiency of run time and information obtained over existing modest data-handling methodology. This multiplication of data-handling capability works because the spectral axis is not coupled to the time axis; therefore, we may freely perform time transformations and spectral transformations independently of each other.

A practical means of spectral multiplexing, such as Hadamard transformation, will involve sequential encodings of the data, with random onset times for each data run. One consequence of this is that phase information is lost. Fortunately, phase information is of little importance for a stationary random process. However, we must be warned that each data run must be long compared to all the correlation times of the system.

The following discussion will be general, but we will use a specific example. We consider the optical spectrum of a complex dynamic system, such as a turbulent flame. Let this spectrum be displayed at the back of a spectrograph. The instantaneous light intensity at any given location at the back of the spectrograph will correspond to the instantaneous concentration of one of the gas species in the flame. We may consider the back plane of the spectrograph to be divided into a large number of spectral channels. Now, let the dispersed light pass through an encoding mask (filter) located in the back plane, and let all the encoded (multiplexed) light be collected by a lens and focused onto a single photodetector (Fig. 1). The time record of this experiment is recorded for a suitable time T, the encoding mask is moved to a new encoding position, and a new time record is recorded, etc.[1] (see Fig. 2).

At each encoding position we will have obtained the time record of a particular partial summation of the spectral intensities over approximately half of the spectral channels. It is the assertion of this work that these time records may be statistically analyzed and then decoded to yield the statistical properties of individual spectral channels.

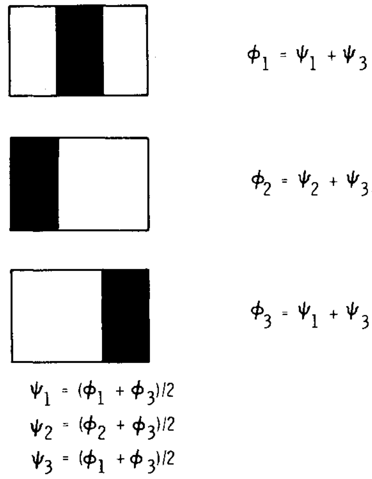

Fig. 3 Three-component example of a Hadamard encoding sequence. The measured (transformed) signals are denoted by ϕ_i, the initial spectral components by ψ_i.

Let us index the spectral channels with the letter j, so that the intensity of the jth spectral element will be $\psi_j(t)$. Each spectral element, or channel, is assumed to be independent of the other spectral elements. We may therefore consider it to be a basis vector $\hat{\psi}_j$, with

$$\hat{\psi}_j = \psi_j \hat{e}_j \tag{1}$$

for a unit spectral vector $\hat{e}_j$. The spectrum as a whole is then a multidimensional vector composed of the basis vectors $\hat{\psi}_j$.

Analysis

Consider a stationary, random process $\vec{\psi}(t)$, with orthogonal spectral elements $\hat{\psi}_j(t)$, where

$$\vec{\psi}(t) = \sum_j \hat{\psi}_j(t) \tag{2}$$

and a stepwise spectrally linear transformation in time of $\vec{\psi}$, given by $\overleftrightarrow{W}(t_i)$ (Fig. 3), where the transformed function $\hat{\phi}_i$ for ith time interval is given by

$$\hat{\phi}_i(t_i') = \sum_j w_{ij}(t_i)\hat{\psi}_j(t_i') \tag{3}$$

where

$$t_i' = t - t_i \tag{4}$$

The transformation $\overleftrightarrow{W}$ has no explicit time dependence, but each of the i summations over j occur sequentially in time, over equal time intervals T, and at onset times t_i. We assume that $\overleftrightarrow{W}$ has an inverse transformation $\overleftrightarrow{V}$, with

$$\overleftrightarrow{V}\overleftrightarrow{W} = \overleftrightarrow{I} \tag{5}$$

or

$$\sum_i \sum_j v_{ji}(t_i) w_{ij}(t_i) = I \tag{6}$$

where v_{ji} and w_{ij} are respectively the matrix elements of $\overleftrightarrow{V}$ and $\overleftrightarrow{W}$. An expression similar to Eq. (3) for $\hat{\psi}_j$ exists only in the case of time averages. For example, if $f[\psi_j]$ is a function of $\hat{\psi}_j$, we may write

$$\int dt f[\hat{\psi}_j(t)] = \int dt f[v_{ji}(t_i)\hat{\phi}_i(t-t_i)] \tag{7}$$

For convenience, we now drop the $(\hat{\ })$ notation, and see that the autocorrelation function $R(\phi_i,\tau)$, defined by

$$R(\phi_i,\tau) \simeq \frac{1}{T}\int_0^T dt \phi_i^*(t)\phi_i(t-\tau) \tag{8}$$

may be expressed as

$$R(\phi_i,\tau) \simeq \frac{1}{T}\int_0^T dt \sum_j w_{ij}^* \psi_j^*(t) \sum_l w_{il}\psi_l(t-\tau) \tag{9}$$

$$= \sum_j \sum_l w_{ij}^* w_{il} R(\psi_j,\psi_l,\tau) \tag{10}$$

where $R(\psi_j,\psi_l,\tau)$ is the cross-correlation function for ψ_j and ψ_l.

This expression can be inverted under the appropriate experimental conditions. We assume that T is greater than any characteristic correlation times of the system, so that the correlation time $\tau + t_i - t_k = \tau\delta_{ik}$, due to the sequential recording of the data. Then we find

$$R(\psi_j,\psi_l,\tau) = \sum_i v_{ji}^*(t_i) v_{li}(t_i) R(\phi_i,\tau) \tag{11}$$

Therefore, we can extract the cross-correlation function for $\psi_j(t)$ and $\psi_l(t)$ from a knowledge of $\vec{\phi}(t)$.

We may easily extend the analysis to obtain the cross-power spectral density $S(\psi_j,\psi_l,\omega)$, given by

$$S(\psi_j,\psi_l,\omega) = \int_{-\infty}^{\infty} d\tau R(\psi_j,\psi_l,\tau) e^{-i\omega\tau}$$

$$\simeq \int_0^T d\tau R(\psi_j,\psi_l,\tau) e^{-i\omega\tau} \tag{12}$$

We find

$$S(\psi_j,\psi_l,\omega) = \int_0^T d\tau e^{-i\omega\tau} \sum_i v_{ji}^*(t_i) v_{li}(t_i) R(\phi_i,\tau) \tag{13}$$

$$= \sum_i v_{ji}^*(t_i) v_{li}(t_i) \int_0^T d\tau e^{-i\omega\tau} R(\phi_i,\tau) \tag{14}$$

$$\simeq \sum_i v_{ji}^*(t_i) v_{li}(t_i) S(\phi_i,\omega) \tag{15}$$

Alternatively, we may begin with the Fourier transforms of $\vec{\psi}$ and $\vec{\phi}$:

$$\vec{\xi}(\omega) = \int_{-\infty}^{\infty} dt e^{-i\omega t}\vec{\psi}(t)$$

$$\simeq \int_0^T dt e^{-i\omega t}\vec{\psi}(t), \quad \omega T \gg 1 \tag{16}$$

$$\vec{\psi}(t) = \frac{1}{2\pi}\int_{-\infty}^{\infty} d\omega e^{i\omega t}\vec{\xi}(\omega) \tag{17}$$

We have similar expressions for $\vec{\phi}(t)$ and its Fourier transform, $\vec{\chi}(\omega)$.

From Eq. (3) we find

$$\chi_i(\omega) \simeq \int_0^T dt_i' e^{-i\omega t_i'}\phi_i(t'), \quad \omega T \gg 1 \tag{18}$$

$$= \sum_j w_{ij}\int_0^T dt_i' e^{-i\omega t_i'}\psi_j(t_i') \tag{19}$$

$$\simeq \sum_j w_{ij}\xi_j(\omega), \quad \omega T \gg 1 \tag{20}$$

Here we again assume that the intervals between the onset times t_i are long compared to the system correlation time scales. Inverting Eq. (20), we find

$$\xi_j(\omega) = \sum_i v_{ji}\chi_i(\omega) \tag{21}$$

Since the cross-power spectral density for ψ_j and the power spectral density for ϕ_i obtained during a time interval T are given by

$$S(\psi_j,\psi_l,\omega) = \xi_j^*(\omega)\xi_l(\omega)/T \tag{22}$$

and

$$S(\phi_i,\omega) = \chi_i(\omega)\chi_i^*(\omega)/T \tag{23}$$

we again obtain Eq. (15). Of course a Fourier transform of Eq. (15) would again give us Eq. (11).

An analysis in terms of pdf's is neither practicable nor useful. However, we may obtain useful results from time-averaged moments. Let us denote time averages by the brackets $\langle\ \rangle$. As in the case of the correlation analysis, if the onset times are separated by a time that is large compared to the correlation times of the system, we may neglect time averages of products between quantities with different onset times. We have

$$\langle\phi_i^2(t_i')\rangle = \left\langle \sum_i \sum_k w_{ij}w_{kl}\psi_j(t_i')\psi_l(t_k')\delta_{ik}\right\rangle \tag{24}$$

$$= \sum_i w_{ij}w_{il}\langle\psi_j(t_i')\psi_l(t_i')\rangle \tag{25}$$

Since we are performing time averages of a stationary random process, the onset time t_i may be ignored, so that we may write

$$\langle\phi_i^2\rangle = \sum_i w_{ij}w_{il}\langle\psi_j\psi_l\rangle \tag{26}$$

We may freely invert Eq. (26) to find

$$\langle\psi_j\psi_l\rangle = \sum_j \sum_l v_{ji}v_{jl}\langle\phi_i^2\rangle \tag{27}$$

A similar analysis applies to a nonstationary but repeatable (nonrandom) experiment, in which the onset times t_i can be set accurately relative to the initiation time of each experiment. In fact, experiments of this type on secular systems have already been undertaken using Fourier transform spectroscopy.[2,3] However, the possibilities for correlation measurements of samples exhibiting random time behavior were not realized in these experiments.

All of these expressions may easily be extended to products of order greater than two and are straightforward to compute. We see that it is possible to extract the richness of detailed information inherent in a time-dependent, multicomponent system by properly analyzing the preserved time record of a multiplexed data processing network. The cost will be some degradation in the S/N ratio. The extent of this degradation will depend on the quality of the multiplexed data processing system. In general, such a system will increase S/N ratio requirements. A minor consideration is that each of the stepped runs must be maintained for a time T, which is long compared to any characteristic time of the system under study. Finally, we note that this analysis may be used in conjunction with modulation spectroscopy to minimize background noise in the acquisition of a spectrum.

References

[1]Harwit, M. and Sloane, N. A., *Hadamard Transform Optics*, Academic Press, New York, 1979.

[2]Manty, A. W., "Infrared Spectroscopic Studies of Transients," *Applied Optics*, Vol. 17, No. 9, May 1978, p. 1347.

[3]Sakai, H. and Murphy, R. E., "Improvements in Time-Resolved Fourier Spectroscopy," *Applied Optics*, Vol. 17, No. 9, May 1978, p. 1342.

Compatibility Conditions from Deformation Displacement Relationship

S. N. Patnaik* and K. T. Joseph†
Vikram Sarabhai Space Centre
Trivandrum, India

Nomenclature

$[B]$	= equilibrium matrix
$[C]$	= compatibility matrix
$\{F\}$	= internal force vector
$[G]$	= concatenated flexibility matrix
IFM	= integrated force method
$[J]$	= displacement coefficient matrix
$\{p\}$	= external load vector
$[S]$	= IFM transformation matrix
SFM	= standard force method
(u,v)	= displacement components
$\{X\}$	= displacement vector
$\{\beta\}$	= deformation vector
$(\epsilon_x,\epsilon_y,\gamma_{xy})$	= plane strain components

Introduction

IN the novel formulation termed the integrated force method (IFM),[1-3] the compatibility conditions (CC) are generated following St. Venant's procedure.[4] In St. Venant's procedure of elasticity, the compatibility conditions are obtained by eliminating the displacements from the strain displacement relationships (SDR). The St. Venant's procedure has now been extended to discrete analysis, and the CC in the IFM are generated by eliminating the displacements from the deformation displacement relationship (DDR). The compatibility conditions thus generated are banded, and the bandwidth is obtained from the element numbering of the discretization.

Basic Theory of Integrated Force Method

In the IFM for discrete analyses, a structure is symbolized as "structure (m,n)," where m is the displacement degrees of freedom (dof) and n the force degrees of freedom (fof). These $(m+n)$ variables must satisfy the following m equilibrium and $(n-m)$ compatibility equation as

Equilibrium equations (EE):

$$[B]\{F\}=\{p\} \tag{1}$$

Compatibility conditions (CC):

$$[C]\{\beta\}=\{0\} \tag{2}$$

The matrices $[B]$ and $[C]$ are independent of design parameters.

In the IFM, Eq. (1) is retained in its original form; however, the deformations $\{\beta\}$ are transformed to forces as $\{\beta\}=[G]\{F\}$. Thus Eq. (2) in forces can be rewritten as

$$[C][G]\{F\}=\{0\} \tag{3}$$

Coupling Eq. (1) to Eq. (3) yields the IFM as

$$\begin{bmatrix} [B] \\ \hline [C]\,[G] \end{bmatrix}\{F\}=\begin{Bmatrix} p \\ \hline 0 \end{Bmatrix} \quad \text{or} \quad [S]\{F\}=\{p\}^* \tag{4}$$

The displacements $\{X\}$ are generated from the forces $\{F\}$ using the following formula,[2,3]

$$\{X\}=[J][G]\{F\} \tag{5}$$

Compatibility Matrix from Deformation Displacement Relationship

St. Venant's formulation of the CC is illustrated taking the example of plane elasticity problem. For the problem, the SDR can be written as

$$\epsilon_x=\frac{\partial u}{\partial x}; \qquad \epsilon_y=\frac{\partial v}{\partial y}, \qquad \gamma_{xy}=\frac{\partial u}{\partial y}+\frac{\partial v}{\partial x} \tag{6}$$

Elimination of displacements from the SDR yield the CC as

$$\frac{\partial^2\epsilon_x}{\partial y^2}+\frac{\partial^2\epsilon_y}{\partial x^2}-\frac{\partial^2\gamma_{xy}}{\partial x\partial y}=0 \tag{7}$$

The two steps of St. Venant's procedure are: 1) establish the SDR and 2) eliminate the displacements from the SDR to obtain the compatibility conditions. The DDR for discrete analysis has been formulated on an energy basis. The internal energy (IE) of structure (m,n) can be written as

$$\text{IE}=\tfrac{1}{2}\{F\}^T\{\beta\}=\tfrac{1}{2}\{X\}^T\{p\}=\tfrac{1}{2}\{X\}^T[B]\{F\} \tag{8}$$

or

$$\tfrac{1}{2}\{F\}^T\Big[[B]^T\{X\}-\{\beta\}\Big]=0$$

Since the force vector is not null, the DDR can be written as

$$\{\beta\}=[B]^T\{X\} \tag{9}$$

Elimination of m displacements from the n DDR given by Eq. (8) yields the $r=(n-m)$ compatibility conditions and the associated coefficient matrix $[C]$.

Bandwidth of the Compatibility Matrix

In the finite-element analysis, the elemental deformations have to be compatible with the neighboring elements; thus the CC are banded. The maximum bandwidth (MBW) of the

Received Jan. 16, 1984; revision received Oct. 2, 1984.

*Engineer, SF, Aerospace Design and Dynamics Group.

†Scientist, SE, Computer Division.